see packet for enclosures

DISTRIBUTION WM-84467
WM S/F 3426.1
WMRP r/f B6985
NMSS r/f
CF
REBrowning
MJBell
JBunting
MRKnapp
LBarrett
LBHigginbotham
HJMiller
RRBoyle
SCoplan
JLinehan
JKennedy
RBCodell
TJMcCartin
DJFehringer
PPBrooks & r/f
PDR
LPDR, B,N,S

JUL 13 1984

Douglas K. Vogt
CorSTAR
7315 Wisconsin Avenue
North Tower, Suite 702
Bethesda, Maryland 20814

SUBJECT: REVIEW COMMENTS ON DRAFT REPORT, "BENCHMARKING OF FLOW AND TRANSPORT CODES FOR LICENSING ASSISTANCE"

Dear Mr. Vogt:

The staff has reviewed the above named draft report received May 24, 1984. This letter summarizes our major comments and recommendations. A set of additional specific comments (listed by page number) and markups of specific pages are included as enclosures. Our general comments relate to major aspects of the report that detract from its technical adequacy and usefulness to the reader.

1. The document should be subjected to thorough technical editing to improve its overall clarity.

   a. References to written reports should be cited for all codes. Citations should be specific throughout the report. For example, on page 5, the dates of the report by Yeh and Ward and "the work of Reeves and Duguid" should be included. This is one way to indicate to the reader that he can find the specifics in the reference section.

   b. Table columns should have clear, informative titles.

   c. Dimensions should be included with numerical values in the text, figures and tables.

   d. Overall clarity of the document is also diminished by the assumption that the reader understands all specialized terms. Brief definitions should be inserted. (See pp 15, 58 of markups)

   e. The problem setups should be clearly and unambiguously described. An example of lack of clarity is found on page 383. See Enclosure 1.

2. The specific version of each code being exercised should be given in Section 1.3 and again in each subsection introducing a code (along with

8411080458

1353

the date, if possible). See also the specific comment for page 3 about SWIFT II in Enclosure 1.

3. A short section on quality assurance measures used in this study should follow Section 1.1 to answer the question of how the rigor of the testing was ensured and documented. See NUREG/CR-3316, page 1-1 for an example of the appropriate level of detail.

4. It is important that a report on several codes should treat the codes evenhandedly. There are several aspects of this report that should be improved to avoid a sense of overall bias.

   a. The analyses of code performances vary in degree of thoroughness. An example that should be expanded upon is found on p 187; "the results are physically reasonable". A more balanced treatment might be achieved by addressing code capabilities directly in each of the discussions of simulation results. In any case, analyses should be more detailed and more nearly at the same level of detail.

   b. Qualitative wording such as "excessive" or "acceptable" should be avoided in comparing simulation results with desired results or results from other codes. See, for example, pp 58, 60, 65, 71, and 75 of the enclosed markups for suggested objective wording.

   c. In comparing codes, a more objective treatment can be achieved by centering the comparison on the code capabilities being tested.

   d. The numerical criterion for a finite difference code is mentioned more negatively for PORFLO (p 111) than for SWIFT (p 377). Please clarify.

   e. Since the description of the code PORFLO does not imply that it can handle a fractured medium, the rationale for exercising the code on problem 9.1 should be given and the description of the simulation results should be accordingly modified. Otherwise it could appear that PORFLO was subjected to an unfair test.

   f. Some codes were afforded what appears to be special treatment (page 164-special feature added to SWIFT, page 316-curvilinear grid for SWIFT, page 377-values changed to match data for SWIFT, page 397-stream tube segments for NUTRAN, page 501-auxiliary program set-up for CCC) that other codes such as PORFLO did not receive. A discussion of the impacts of such modifications on the assessment of

OFC	:WMRP:mkg	:WMRP	:WMRP	:	:	:	:
NAME	:PPBrooks	:DJFehringer	:JJLinehan	:	:	:	:
DATE	:84/07/13	:7/ /84	:7/ /84	:	:	:	:

relative applicability of codes can contribute to the objectivity of the report.

5. The authors should give the basis for modifications such as described on page 16 in sufficient detail to make it clear whether the modification can or should be repeated. Do the modifications solve the problem or bypass it? When and how should they be used in solving more complex problems? These questions should be addressed briefly where appropriate.

Please address the general and specific comments in your revision of the draft report. Enclosure 3 is included for your information.

The action taken by this letter is considered to be within the scope of the current contract NRC-02-81-026. No changes to cost or delivery of contracted products are authorized. Please notify me immediately if you believe this letter would result in changes to cost or delivery of contract products.

Sincerely,

"ORIGINAL SIGNED BY"

Pauline P. Brooks
Repository Projects Branch
Division of Waste Management
Office of Nuclear Material
Safety and Safeguards

Enclosures:
1. Specific Comments
2. Markups
3. Analytical Model for Repository Temperature

cc: Peter Cukor
Sharon Wollett

Record Note: This work was coordinated with R. B. Codell (WMGT) and T. J. McCartin (WM Branch, RES) and incorporates comments dated July 2, 1984 and June 20, 1984, and discussed subsequently.

OFC	:WMRP:mkg ppb	:WMRP	:WMRP	:	:	:	:
NAME	:PPBrooks	:DJFehringer	:JJLinehan	:	:	:	:
DATE	:84/07/13	:7/13/84	:7/ /84	:	:	:	:

Ltr to Voss
fm. Brooks
7/13/84
B6985

ENCLOSURE 1

Specific Comments on Draft Report
"Benchmarking of Flow and Transport Codes for Licensing Assistance"
(B6985)

Page 3 - The report should be consistent throughout as to whether SWIFT or SWIFT II was used. The code description implies SWIFT II.

Page 5, last 2 lines - "The work of Reeves and Duguid" is unreferenced.

Page 6, Section 1.3.7 - No reference is given for the code CCC here or on page 470.

Page 15, under item 2 - Define "block centered approach." Why is this important? It hits the reader out of the blue with no frame of reference.

Page 15 - USGS3D was discretized in a unique way. What led the authors to decide upon this choice?

Page 33, Section 2.4.2 - Why was the initial value of the storage coefficient allowed to vary from 0.003 to 0.006 for USGS 3D? Why did Pinder and Brehehoeft do this? Did this involve a program modification? If so were all codes handled fairly in this regard? Could you have done it if you were not intimately familiar with the code?

Page 63, Section 3.3.2.1 - Why is equivalent isotropic transmissivity calculated as shown? What units does the quantity 10^{-7} have?

Page 67 - Results of PORFLO still look quite good. Are we splitting hairs?

Page 67 - The results of the comparison look good, and don't appear to deserve much criticism.

Page 96, Line 12 - Something is missing from the equation.

Page 99 - It appears that the time step criteria were violated for this simulation. What is the effect on the results?

Page 107 - The INTRACOIN parameter P1 should be "100 or infinity", thereby making dispersion length equal to .5m and making the criterion mentioned on page 111 less restrictive.

Page 117, Table 3.19d - the computed and converted concentrations for time = .300E5 are highly suspect, since they differ from other values in the table by 12 orders of magnitude.

Page 124, Footnote - alpha missing.

Page 125, line 14 - lambda missing

Page 136 - The Peclet number is constant but the dispersion length should vary over the three zones (See discussion of page 403 of draft report).

Page 146, First Line - Sentence repeats

Section 3.10 - General - It is difficult to interpret from what you said, how this code was set up to do the fracture flow problem. Also, you refer to the x, z dimensions in Fig. 3.24 but to x, y in table 3.28. How was the velocity in the fractures specified? How can an independent investigator follow your example?

Page 167 - Table 4.3-3 is not easy to understand. To what do your column headings refer? Figure 4.3-2 is also less than clear.

Page 191 - Section 4.6 - General - This is an interesting application of SWIFT, executed by Mark Reeves and presented at the Spring 1984 AGU conference. This is a case, however, of the expert (code author) who is very familiar with the code, and who can do extraordinary things with it. It doesn't appear that an equal effort went into the PORFLO or USGS 3D simulations.

Furthermore, the solution is an inappropriate application of SWIFT for the purpose of benchmarking. The two well doublet is easy to map into a curvilinear space because there is a well known solution for stream function and potential. The SWIFT simulation naturally works well, because velocity is parallel to the streamlines, and grid blocks are concentrated in the area near the wells. Even a very simple model would be expected to work here.

Unfortunately, any real problem would be difficult or impossible to map in such a manner, so the good agreement of SWIFT with the analytic solution loses its significance. It would have been much more meaningful to set up SWIFT in its normal cartesian mode for this problem, because this would show the complications of defining point sources and sinks in a cartesian grid. Also, the results would bear more resemblance to the results of USGS3D and PORFLO.

The rationale for the choice of coordinates should be expanded. The usefulness of this approach for benchmarking and to the independent investigator who uses the code in a more complex situation should be addressed.

The side-by-side comparison of the curvilinear and cartesian coordinate problem for the well doublet presented in Section 5.3 was the most useful of the studies, since it pointed to the difficulties of representing point sources in a cartesian grid.

Page 207, last 2 lines - Your results on the thermal profile with the 2-D simulation are questionable. An analytical study by the staff shows that there would be a significant error introduced by neglecting heat transfer in the third dimension. The attached NRC memorandum summarizes a study of hypothetical a basalt waste repository very similar to yours. The error demonstrated in Figure 3 of that memo would be similar to the error committed in your study by neglect of the third dimension. Give details of the dimensional considerations which you employed to justify the 2-D approximation. This same concern would apply to problem 7.1, which is also a 2-D representation.

Page 267, Lines 5 and 6 - Do you mean "dispersivity" for "dispersion"? Line 10 - To what does the term "dimensional effects" pertain?

Page 276, first equation - T_1 is not defined, unless the subscript was left off below.

Page 276 - middle of page - The explanation of "pseudo steady state is confusing - describe why this equation is pseudo steady state, and why the form of the equation was chosen this way.

Page 279 - Explain how W_1 was evaluated from the SWIFT output.

Page 281 - Last sentence, first paragraph under 5.2.3. It is difficult to understand why the second case is called "pseudo - steady state" if the complete transient analysis is used. Please expand your explanation.

Page 282 - Figure 6 is not clear. Is there a typo?

Page 283 - Give bases for deriving equation 5.2-10.

Page 293 - Table 5.2.6 - There is no information given telling <u>what</u> the results are. Presumably you mean the values of W_1.

Page 285 - Several problems in this section suggest that the dual porosity version of SWIFT was used. Be sure to note when and if the dual porosity feature was employed.

Page 288 - Lines 10-11 - On what basis do you conclude that the length is sufficient to simulate infinity? Did you try other lengths?

Page 304 - Comparison with INTRACOIN results would be aided by a graph of the results of SWIFT and INTRACOIN.

Page 315 - The adjustment of the Np 237 inventory in the near field is inadequately documented. Describe this adjustment in more detail.

Page 370 - Was dual-porosity SWIFT used for this problem? Your description of the code setup does not make this clear.

Page 376 - Are D* and D_d the same?

Page 377 - Last sentence - Was the adjustment to the molecular diffusion a computational expedient? What was the basis for this change? It seems hard to believe that the molecular diffusion coefficient would make much of a difference in the results because it is generally small compared to the overall dispersion.

Page 383 - It is unclear whether data or the results of Bibby's model were used for the SWIFT run. Adjustment of the SWIFT transmissivities to better match Bibby's results is irrelevent, and adds nothing to the benchmarking. The presentation of this problem lacks clarity. The boundary and initial equations should be clearly stated.

Page 385 - Last Paragraph - This paragraph implies that NUTRAN is a one-dimensional pipe flow model. Section 6.3 looks at a 2 dimensional problem with 5 stream tubes. It is not clear from your writeups whether or not NUTRAN can handle multiple pathways, or if problem 6.3 was pieced together from separate runs of NUTRAN. Please amplify your discussion on the uses and limitations of NUTRAN.

Page 397 - Last Paragraph - The discussion on dividing the stream tubes so that they have an approximately uniform ground water speed in each segment is not clear. The groundwater velocity in each stream tube would vary along the streamtube, as well as between streamtubes. Do you mean by your statement that the length of each segment was chosen so that the travel time across its length was a constant? Please clarify.

Page 403 - Since this result was not compared to any other cases or analytical results, how can its reliability be quantified?

Page 411 - Line 8 - A Peclet number of 0.5 is unreasonably low. Is there a physically reasonable system which would relate to this value?

Page 421 - It is unclear whether or not the correct values for dispersion length in the three zones were used (See comment for page 136).

Page 454 - That fact that one can change simulation results by changing parametric values does not contribute to the benchmarking. The change in K_s from 450 cm/d to 100 cm/d should include some technical discussion as to why.

Page 458 - Why didn't the authors try a smaller grid and/or time increment to examine the overshoot/numerical dispersion problems?

Page 486 - Another example of the use of the natural coordinate system, which the staff contends does not realistically evaluate the model. Please expand the rationale for the choice of coordinate system in the context of this criticism.

better test these features. The results of the hypothetical problem runs are intended to serve as a basis for comparison with results from other codes.

1.2 SCOPE OF THIS REPORT

This report is intended to serve as a sequel to the report "Benchmark Problems for Repository Siting Models" (NUREG/CR-3097). Both reports consider a set of problems applicable to the testing of codes which may be used to aid in repository siting. Specifically, they are intended to be used to provide a basis for evaluating codes that simulate the uncoupled or coupled processes of fluid flow, contaminant transport and/or heat transfer. Other physical processes important to the evaluation of a potential site, such as geomechanical response will be considered in separate NUREG reports. Coupled processes where geomechanical response is simulated will also be considered in other reports. A discussion of the codes benchmarked in this report is provided below. For a more in-depth description, the reader is referred to the model summary report by Thomas et al. (1982).

Not in references file Include!

1.3 CODES BENCHMARKED

1.3.1 USGS3D

USGS3D is a three-dimensional finite difference code designed to simulate ground-water flow through saturated porous media. The code is capable of evaluating heterogeneous and anisotropic media with irregular boundaries and can be used in both fully three-dimensional or quasi-three-dimensional modes. The quasi-three-dimensional mode evaluates a three-dimensional layered system by representing aquifers as a sequence of two-dimensional areal models coupled by terms representing steady-

This table should agree with actual contents of report

Table 1.1. Codes and Problems to be Solved.

Code	Problems
SWIFT	3.2, 3.4, 3.5, 3.6, 5.2, 5.3, 7.1, 8.2, 8.4
NWFT/DVM (generalized version)	8.1, 8.2, 8.3, 8.4
NUTRAN	8.1, 8.2, 8.3, 8.4
USGS3D	3.2, 3.4, 3.5
SWIFT	6.1, 9.1, 9.2, 9.3, 10.1, 10.2
PORFLO	3.2, 3.4, ~~3.5~~ 5.1a, 5.1b, 5.2, 5.3, 8.1, 8.2, 8.3, 8.4
FEMWATER	4.1, 4.2, 4.3
FEMWASTE	10.1, 10.2
CCC	3.2, 5.1a, 5.1b, 5.2, 5.3

Problems and problem numbers correspond to those in the benchmark problem report by Ross et al. (1982).

2.0 BENCHMARKING OF USGS3D

2.1 PROBLEMS SOLVED

Four isothermal ground-water flow problems were solved using the USGS3D finite difference code. These problems are as follows:

- Problem 3.2: Transient radial flow to a fully penetrating well in a leaky confined aquifer system.
- Problem 3.3: Transient radial flow to a fully penetrating well in an anisotropic confined aquifer.
- Problem 3.4: Areal flow in the Musquodoboit river basin.
- Problem 3.5: Three-dimensional steady flow in a hypothetical basalt repository system.

2.2 PROBLEM 3.2: FLOW TO A WELL IN A LEAKY AQUIFER SYSTEM

This problem is concerned with the process of transient flow to a well fully penetrating a uniform aquifer overlain by a confining layer or aquitard with a water source (aquifer) above (Figure 2.1). The flow in the aquifer is assumed to be radial and the flow in the aquitard is assumed to be vertical. Such an assumption has been found to be valid (Neuman and Witherspoon, 1969) when the hydraulic conductivity of the aquifer is at least two to three orders of magnitude greater than that of the aquitard.

2.2.1 Problem Statement and Objectives

This problem is selected to test the capability of the code to handle transient flow in a leaky aquifer system taking into account storage in the confining layer.

The problem is governed by the following equations:

$$K \left(\frac{\partial^2 s}{\partial r^2} + \frac{1}{r} \frac{\partial s}{\partial r} \right) + \frac{K'}{b} \frac{\partial}{\partial z} s'(r,b,t) = S_s \frac{\partial s}{\partial t} \qquad (2.1)$$

and

$$K' \frac{\partial^2 s'}{\partial z^2} = S_s' \frac{\partial s'}{\partial t} \qquad (2.2)$$

where

s = drawdown in the aquifer (L)

r = horizontal radial distance from well center (L)

K' = confining bed hydraulic conductivity (Lt^{-1})

K = aquifer hydraulic conductivity (Lt^{-1})

where for the short time solution (see Figure 2.2),

$$W = W(u,\beta') = \int_u^\infty \frac{e^{-y}}{y} \operatorname{erfc}\left[\frac{\beta'\sqrt{u}}{\sqrt{y(y-u)}}\right] dy \qquad (2.6a)$$

and u and β' are dimensionless parameters defined as

$$u = \frac{r^2 S}{4Tt}$$

$$\beta' = \frac{r}{4}\sqrt{\frac{K'S'_s}{TS}}$$

in which T and S are the aquifer transmissivity and storage coefficient, respectively, (i.e., T = Kb, S = S_sb).

For the long time solution,

$$W = W(u',\frac{r}{B}) = \int_{u'}^\infty \frac{1}{y} \exp\left(-y - \frac{r^2}{4B^2 y}\right) dy \qquad (2.6b)$$

where r/B is a dimensionless parameter defined as

$$\frac{r}{B} = \frac{r}{\sqrt{Tb'/K'}}$$

$$u' = (1 + S')3S)u$$

2.2.2 Input Specifications

1. Physical parameters

Two simulations were performed using the USGS3D code. The values of the physical parameters used were carefully selected to ensure that regions of validity of the two asymptotic solutions (Figure 2.2) lie

well within the simulation time period. These parameters are as follows:

$$T = 0.05\ m^2/s \quad , \quad S = 0.005$$
$$K' = 10^{-5}\ m/s \quad , \quad b' = 50\ m$$
$$S_s' = 0.0016\ m^{-1} \quad , \quad Q = 6.283\ m^3/s$$

To check the finite difference results, the drawdown versus time relationship at r = 117.4 m was computed using the analytical solutions given in equations (2.5) and (2.6). The values of β', r/B, and u' corresponding to the given values of physical parameters are $\beta' = 0.235$, r/B = 0.235, and u' = 6.33u, respectively.

2. Discretization data

Two different rectangular grids were set up and used to obtain the short time and long time solutions, respectively. The grids differed in the degree of discretization in the vertical direction. In the early time range where storage effects are dominant, the aquitard must be finely discretized to accurately represent the effects of the steep gradient across it. In reference to the discretization procedure, it should be noted that USGS3D utilizes a block centered approach.

For the run applicable to early time (Run #1) the z spacings are as follows:

Block k	1	2	3	4	5	6	7	8	9	10	11
Δz_k, m	2	46	2	2	3	4	6	9	12	14	2

where blocks 1, 2, and 3 represent the underlying aquifer, blocks 4 through 10 are the aquitard, and block 11 is the overlying water source.

Table 2.1a. Comparison of USGS3D Simulation Results with Hantush's Solutions for Transient Flow to a Well in Leaky Aquifer with Storage in the Overlying Aquitard (Grid #1).

Time (10^3 sec)	Drawdown at r = 117.4 m	
	Analytic	USGS3D (weighted average)
0.44	1.94	2.08
0.72	3.52	3.55
1.12	5.26	5.20
1.69	7.08	6.95
2.49	8.90	8.75
3.62	10.73	10.58
5.22	12.56	12.41
7.48		14.23
10.67		16.06
15.19		17.87
21.58		19.67
30.62		21.45
43.40		23.21
61.46		24.94
87.01		26.62
123.13	28.77	28.18
174.20	30.14	29.56
246.42	31.08	30.67
348.54	31.63	31.44
492.93	31.90	31.94
697.11	32.01	32.20
958.81	32.01	32.32
1394.04	32.01	32.32

2.3 PROBLEM 3.3: FLOW TO A FULLY PENETRATING WELL IN AN ANISOTROPIC CONFINED AQUIFER

2.3.1 Problem Statement and Objectives

This problem was selected to test the capability of the code to simulate fluid flow in anisotropic porous media. The problem concerns transient ground-water flow to a pumped well fully penetrating an anisotropic but homogeneous confined aquifer. This problem may be described by the following equation:

$$T_{xx}\frac{\partial^2 s}{\partial x^2} + 2T_{xy}\frac{\partial^2 s}{\partial x \partial y} + T_{yy}\frac{\partial^2 s}{\partial y^2} + Q\delta(x)\delta(y) = S\frac{\partial s}{\partial t} \qquad (2.8)$$

where

s = drawdown in the aquifer (L)

T_{xx}, T_{yy}, and T_{xy} = components of the transmissivity tensor (L^2T^{-1})

Q = well discharge (L^3T^{-1})

S = storage coefficient.

The initial and boundary conditions associated with equation (2.8) may be expressed as:

$$s(x,y,0) = 0 \qquad (2.9a)$$

$$s(\pm\infty,y,t) = 0 \qquad (2.9b)$$

$$s(x,\pm\infty,t) = 0 \qquad (2.9c)$$

Picture of problem geometry needed.

Table 2.4 Hydraulic Properties of Various Materials in the Hypothetical Basalt System.

Zone Type	Thickness (m)	Hydraulic Conductivity (m/yr)
Aquifer 1	20	2×10^{-6}
Aquitard	100	3×10^{-11}
Aquifer 2	20	10^{-6}
Crushed Zone	140	10^{-5}
Coarse Sediments	20	10^{-4}

problem were solved using vertical instead of horizontal slices. Generally, vertical slicing has been shown to reduce the number of iterations in half in problems where horizontal layers of contrasting hydraulic conductivities exist. To implement this type solution scheme only minor changes would have to be made to USGS3D.

For comparative purposes, the steady-state results for horizontal planes z = 7.5 m and z = 132.5 m for both simulations are tabulated in Tables 2.6 and 2.7.

The drawdown values calculated by PORFLO are generally within — % of the analytic solution, with a maximum difference of — % at — sec.

3.2 PROBLEM 3.2: FLOW TO WELL IN A LEAKY AQUIFER SYSTEM

3.2.1 Problem Statement and Objectives

The problem statement and objectives of the test have been described in Section 2.2.1.

3.2.2 Input Specifications for PORFLO

A transient simulation of the flow problem was performed using the PORFLO code. The well radius was assumed to be 0.8 ft. The hydraulic properties and the well discharge used in the simulation are identical to those given in Section 2.2.2. The spatial and temporal discretization data selected for PORFLO are presented in Table 3.1. Note that with the given value of the initial time step, the remaining time steps were generated automatically by the code.

3.2.3 Simulation Results

The problem was solved for 50 time steps. Weighted average values of drawdown at r = 117.4 m are presented in Table 3.2. These drawdown values are plotted in Figure 3.1. ~~As can be seen, there is acceptable agreement between the numerical and the analytical solutions. To further assess the accuracy of the PORFLO code, one may compare~~ A comparison of the plot in Figure 3.1 with that in Figure 2.4. ~~Evidently,~~ shows that the result given by PORFLO is ~~considerably~~ less accurate than the result given by USGS3D, although similar grid spacings were used in running both codes and more time steps were used in running PORFLO. This may be attributed to the different matrix solution techniques used in the two codes. The PORFLO code employs the noniterative Peaceman-Rachford ADI (Alternating Direction Implicit) technique. Although the ADI technique requires less

computational effort per time step than common methods such as SIP (Strongly Implicit Procedure) and SSOR (Slice Successive Overrelaxation), the ADI technique ~~technique~~ usually requires an excessive number of time steps to achieve an accurate solution. In this case, the USGS3D code, which employs the iterative SIP technique, gives a more accurate answer.

larger?

What is the bottom line? Does the increased number of time steps offset the reduced computing per step? How do USGS3D and PORFLO compare in terms of accuracy per dollar of computer time?

3.3.3 Simulation Results

The numerical results obtained are presented in Table 3.4. Converted values of drawdown are plotted against time in Figure 3.2. Also depicted is the corresponding analytical solution. It can be seen that there is overall agreement between the analytical and the numerical solutions. However, upon comparing Figure 3.2 with Figure 2.5 of Chapter 2, it is evident that the accuracy of the numerical result from the PORFLO is not as good as the accuracy of the result from USGS3D. The reason for this is again the different time stepping schemes employed by the two codes. The PORFLO code employs the non-iterative ADI (Alternating Direction Implicit) scheme which normally requires many more time steps than the fully-implicit time stepping scheme employed by USGS3D to obtain comparable accuracy.

ρ_m, c_m = density and heat capacity of the combined medium;

t = elapsed time;

c_R = heat capacity of the confining bedrock; and

ρ_R = density of the bedrock.

Note that the normalized temperature is defined as:

$$u = (T-T_0)/(T_1-T_0) \tag{3.3}$$

where T is the temperature in the aquifer, T_1 is the temperature of the injected fluid, and T_0 is the ambient temperature.

Equations (3.1) and (3.2) were solved analytically by Avdonin (1964) subject to the following initial and boundary conditions:

$$u(r,0) = 0 \quad \text{for } r > 0 \tag{3.4a}$$

$$u(0,t) = 1 \quad \text{for } z = 0,\ t > 0 \tag{3.4b}$$

$$\lim_{r^2 + z^2 \to \infty} u = 0 \tag{3.4c}$$

The analytical solution takes the form:

$$u(\omega,\tau) = \frac{1}{\Gamma(\nu)} \left[\frac{\omega^2}{4\tau}\right]^{\nu} \int_0^1 \left\{\exp\left(-\frac{\omega^2}{4\tau s}\right) \operatorname{erfc}\left(\frac{\alpha s\sqrt{\tau}}{2\sqrt{1-s}}\right)\right\} \frac{ds}{s^{\nu+1}} \tag{3.5}$$

where

$$\nu = \frac{Qc_w\rho_w}{4\pi b K_m}, \quad \omega = \frac{2r}{b}, \quad \lambda = \frac{4K_m t}{c_m\rho_m b^2}, \quad \alpha = \left(\frac{K_r c_r \rho_r}{K_m c_m \rho_m}\right)$$

and $\Gamma(\nu)$ is the gamma function.

3.4.2 Input Specifications

The stated heat flow problem was solved using PORFLO. The values of the physical parameters used in the simulation are listed in Table 3.5. Darcy velocity was computed from $v = Q_I/2\pi rb$ where, for PORFLO, the r value is at the left edge of the nodal block. The spatial and temporal discretization data used in the finite difference simulation are provided in Table 3.6. Note that symmetry of the flow region was taken into account by discretizing only the cap rock and the upper half of the aquifer. It was necessary to adopt a finite well radius ($r_w = r_1$) in order to avoid difficulties in applying the code to this problem. In addition, values of the time steps were kept rather small to ensure numerical stability. To check the numerical result, the Avdonin solution was used to compute the breakthrough curve at $r = 37.5$ m, and the temperature profile at $t = 10^9$ sec.

3.4.3 Simulation Results

Two cases were simulated; one in which thermal conduction in the confining bedrock was taken into account, and the other in which this thermal conduction was neglected. The purpose of the second case was to assess the importance of heat transfer in the confining bedrock. The second simulation was achieved simply by disregarding the bedrock in the spatial discretization.

For a time value of 10^9 sec, a comparison of temperature profiles obtained from the two numerical simulations and the analytical solution is shown in Figure 3.4. As can be seen, ~~the overall accuracy of the numerical results is acceptable~~. ~~Apparently~~, much better agreement between the numerical and the analytical solutions was obtained for case 2.

Also evident is the fact that there is quite a substantial difference between the temperature profiles corresponding to cases 1 and 2. This indicates that the heat transfer in the confining layers was significant.

A comparison of breakthrough curves at r = 37.5 m is depicted in Figure 3.5. The agreement between the numerical and the analytical solutions is not as good as one would expect. The main reason for this is the limitation of the ADI matrix solution and time-stepping scheme employed in the PORFLO code. As pointed out earlier in Section 3.2.3, such a scheme may require ~~an excessive~~ a large number of time steps to yield an accurate solution.

For reference purposes, the results of the numerical and analytical computations are also provided in Tables 3.7 and 3.8.

What is the basis for saying this? It looks like the results may be sufficiently accurate for most purposes.

The difference in placement and slope of the curves for the two cases shows that the heat transfer to the confining layers is significant. Case 1 shows better agreement with the analytical solution. As the case 2 analytical solution has a greater slope, the greater inaccuracy of the numerical solution is as expected.

A comparison of breakthrough curves at x = 600 m for cases 1 and 2 are shown in figures 3.8 and 3.9 respectively. The curves shown are for the second order solution and yet the agreement is not as good as expected. The main reason for this is the limitation of the ADI matrix solution and time-stepping scheme employed in the PORFLO code. As pointed out in Section 3.2.3, such a scheme may require an excessive number of time steps to yield an accurate solution. The disagreement for case 1 is greater, perhaps because of the numerical difficulties in simulating heat transfer to the confining layers.

For reference purposes, the results of the temperature profile numerical and analytical computations are also provided in Tables 3.11 and 3.12.

Table 3.13. Values of the Physical Parameters for Problem 5.2.

Parameter	Value
Distance between wells, 2a	300 ft
Flow rate of wells, Q	60,000 ft^3/d
Aquifer thickness, b	50 ft
Effective porosity, ϕ	0.3
Injection temperature, T_I	60°F
Initial temperature, T_0	45°F
Density of water, ρ_w	62.4 lb/ft^3
Heat capacity of water, c_w	1 BTU/(lb °F)
Specific volume heat capacity, $\rho_m c_m$	40 BTU/(ft^3 °F)
Aquifer thermal conductivity coefficient, K_m	0 BTU/(ft/d °F)

Case 1: K_R = 6933.3 BTU/(ft/d °F), $\rho_R c_R$ = 40 BTU/(ft^3 °F)
(λ_D = 0.3)

Case 2: K_R = 693.33 BTU/(ft/d °F), $\rho_R c_R$ = 40 BTU/(ft^3 °F)
(λ_D = 3.0)

Case 3: K_R = 69.333 BTU/(ft/d °F), $\rho_R c_R$ = 40 BTU/(ft^3 °F)
(λ_D = 30.0)

Case 4: K_R = 6.9333 BTU/(ft/d °F), $\rho_R c_R$ = 40 BTU/(ft^3 °F)
(λ_D = 300.0)

?

BTU/(ft d °F)

3.6.4 Simulation Results

Computed values of temperature at the production well were non-dimensionalized and plotted in Figure 3.13 against the dimensionless time, t_D. It can be seen that the numerical solution agrees reasonably well with the analytical solution until a time value that corresponds to $t_D = 20$ is reached. At larger time values, the agreement becomes poorer and eventually at t_D equal to approximately ~~40~~ 400, the numerical solution becomes unstable and exhibits unbound exponential oscillations. The numerical instability is primarily due to the fact that the time stepping procedure employed by the PORFLO code is a non-iterative alternating direction implicit (ADI) matrix solution scheme. As pointed out earlier, such a scheme is often restricted by the size of time steps. For this problem, one would have to use ~~an excessive~~ a very large number of time steps (probably on the order of several thousand) to avoid the numerical difficulty.

For reference purposes, the results given by the PORFLO code are also provided in tabular form (see Table 3.15).

Figure 3.13 should give the λ_D values for the two analytic solution curves.

Exit boundary condition

E1: Semi-infinite extent

$$c_r(\infty,t) = 0 \tag{3.19a}$$

E3: Finite system of length L

$$\frac{\partial r_c}{\partial x}(L,t) = 0 \tag{3.19b}$$

where ϕ is the effective porosity, F is the flow cross-sectional area, T is the leach duration, and $I_r(t)$ is the total inventory of nuclide r at time t. The function $I_r(t)$ satisfies Bateman's differential equation,

$$\frac{d}{dt} I_r(t) = -\lambda_r I_r(t) + \lambda_s I_s(t) \tag{3.20}$$

with given initial values of I_r^o. Analytical solutions of the stated transport problem can be found in Harada et al. (1981).

Twelve cases are to be solved. The physical parameter values to be used are given in Table 3.16. Note that the twelve cases are defined by combining three dispersivity (or Peclet number) values, two inventories, and two sets of retardation factors. If the exit boundary condition E3 is used, the system L is to be assumed as 500 m.

3.7.2 Input Specifications for PORFLO

Only Eight of the twelve cases mentioned can be handled by the PORFLO code. The parameter sets for the eight cases that were solved are summarized in Table 3.17. The remaining four cases are those for

3.7.3 Simulation Results

To enable the simulation results from PORFLO to be used in the INTRACOIN comparative study of nuclide transport codes, concentration values at the outlet, which correspond to x = 500 m, were processed. The breakthrough curves are presented in Figures 3.10 and 3.11 for cases 1-4 and cases 5-8, respectively. The peak release rates at corresponding time values are summarized in Table 3.18. These results fall well within the range of breakthrough curves presented in INTRACOIN's level one report and the report prepared by INTERA (1982). For reference purposes, the lists of time versus computed and converted concentration values are provided herein (see Tables 3.19a-3.19h).

retardation factors are constant. To accommodate the time-dependent concentration boundary condition at the inlet, the same procedure described in Section 3.5.2 was also adopted for this problem.

3.9.3 Simulation Results

To enable the simulation results for PORFLO to be used in the INTRACOIN comparative study of nuclide transport codes, concentration values at the outlet section (x = 500 m) were processed. The breakthrough curves are presented in Figure 3.22. For cases 1 and 2, the peak release rates are approximately 0.591×10^{-5} and 0.861×10^{-5} ci/yr, and these peaks occur at time values of 0.132×10^{6} and 0.48×10^{5} years, respectively. These curves compare reasonably well with the set of breakthrough curves presented in INTRACOIN's level one report. For reference purposes, numerical values of concentration are provided in Tables 3.26a and 3.26b.

How well? Need to be more specific. Where is comparison of breakthrough curves?

9.5 Problem 5.2: HEAT TRANSPORT BETWEEN INJECTION AND WITHDRAWAL WELLS

9.5.1 Problem Statement and Objectives

The problem statement and objectives of the test have been described in Section 3.6.1.

9.5.2 Input Specifications

The movement of a thermal front in a well doublet system was solved using CCC. The values of the physical parameters used in the simulation are the same as described in Section 3.6.2 and summarized in Table 9.5-1. The temperature changes (thermal breakthrough) at the withdrawal well depends on the thermal front displacements along stream channels in the aquifer and on the heat leakage to the confining cap rock and bed rock. Four cases of different thermal conductivity of the confining units, as expressed by the dimensionless parameters λ_D (Eq. 3.16b), were simulated in this test.

For the two-dimensional steady flow field in the aquifer, the flow potential ϕ and the stream function ψ can be determined by the complex potential theory:

Subscripts ?

$$\phi + i\psi = \frac{Q}{2\pi b} \ln(r_1 e^{i\theta}) - \frac{Q}{2\pi b} \ln(r_2 e^{i\theta}) \qquad (9.5\text{-}1)$$

where Q is the flow rate, b is the aquifer thickness. The r_i, θ_i are the polar coordinates centering around two wells, i=1,2, respectively, as illustrated in Figure 5.4-1. In terms of the dimensionless potential η an the dimensionless stream function ξ of Section 4.6.3:

$$\phi + i\psi = \frac{Q}{2\pi b} (\eta + i\xi) \qquad (9.5\text{-}2)$$

with

$$\eta = \ln\left(\frac{r_2}{r_1}\right) \quad ; \quad \xi = \theta_2 - \theta_1 \quad . \qquad (9.5\text{-}3)$$

ANALYTICAL MODELS FOR TEMPERATURE SURROUNDING A HLW REPOSITORY

by Richard Codell, WMGT
Division of Waste Management, NMSS

Introduction

Heat generated from a waste repository will be transported from the repository by conduction through the rock and to a lesser extent by convection by flowing water. The conditions for which the convective heat transfer could be neglected were explored in Ref. 1. For many, if not most cases of HLW repositories, convective heat transfer would be much less important than conductive heat transfer.

A useful extension of the analytical heat transfer models employed in Ref. 1 has been made which allows the calculation of the temperature of the rock as a function of time and distance from a rectangular, thin plate heat source in an infinite, uniform, 3-dimensional medium. Such an analysis is useful for evaluating the extent of penetration of isotherms into the medium for an estimate of the dimensions of the disturbed zone. The model is also useful for checking more complicated models, e.g., testing their sensitivity to different boundary conditions.

Consider the repository represented in Figure 1. The waste is uniformly distributed in a horizontal plane L meters long and W meters wide, and is infinitesimally thin. Heat is being generated at a rate $H = H_o f(t)$ joules/year per square meter of repository area.

The repository is located in a rock which has uniform properties in all directions. The thermal conductivity is k joules/(meter-sec-°C). The heat capacity is ρC_p joules/(m^3-°C).

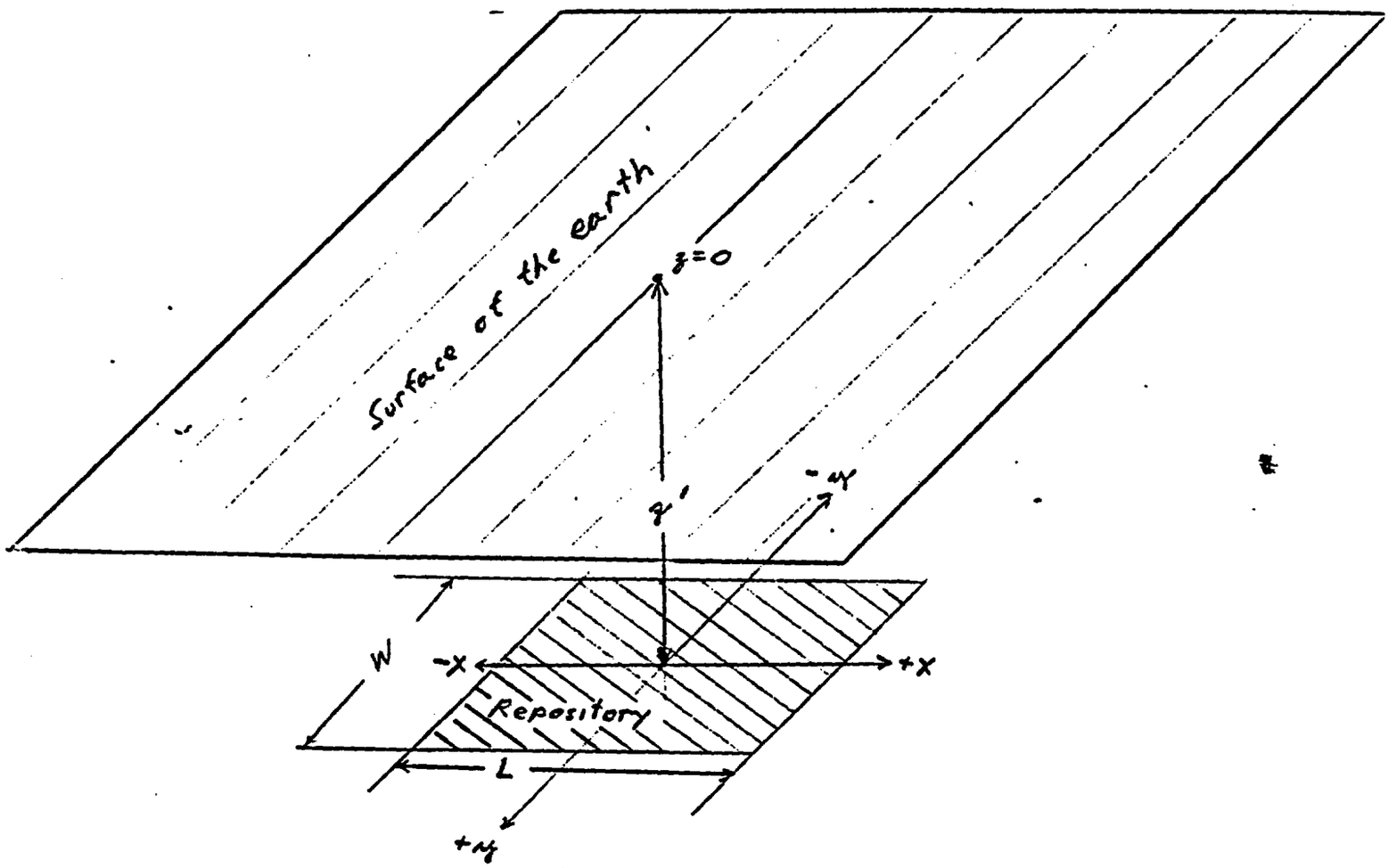

FIGURE 1 - HIGH LEVEL WASTE REPOSITORY

The repository plane is located z' meters below the surface of the earth. Heat is being lost from the earth's surface to the atmosphere at a rate proportional to the difference between the surface temperature and the ambient temperature:

$$q \frac{(\text{joules})}{m^2\text{-yr}} = K_e (T_o - T_A) \qquad (1)$$

where K_e = equilibrium heat transfer coefficient joules/m^2-yr-°C

T_o = temperature of the ground surface

T_A = ambient atmospheric temperature.

The coefficient K_e can be estimated from the formula used for cooling of bodies of water, with an adjustment for the lower evaporation from land surface (Ref. 2). The coefficient K_e is expected to be approximately in the range 2×10^8 to 4×10^8 j/(m^2-yr-°C).

A geothermal gradient may exist, but there would be no loss of generality in considering the temperature calculated to be that measured above the normal background temperature. This can be demonstrated by the following arguments.

Consider the naturally ocurring ambient rock temperature T_B to be

$$T_B = T_A + Gz \ , \qquad (2)$$

where T_A = is the ambient atmospheric temperature at the ground surface (for simplicity, ignore daily or seasonal variations in temperature)

G = is the geothermal gradient (a constant), °C/m.

The temperature difference above ambient rock temperature is defined

$$\theta = (T - T_B) \ . \qquad (3)$$

The equation for heat transfer in a uniform isotropic medium is (Ref. 3):

$$\frac{\rho C_p}{k}\frac{\partial T}{\partial t} = \frac{\partial^2 T}{\partial x^2} + \frac{\partial^2 T}{\partial y^2} + \frac{\partial^2 T}{\partial z^2} \tag{4}$$

If G is a constant, then

$$\frac{\rho C_p}{k}\frac{\partial \theta}{\partial t} = \frac{\partial^2 \theta}{\partial x^2} + \frac{\partial^2 \theta}{\partial y^2} + \frac{\partial^2 \theta}{\partial z^2} \tag{5}$$

The boundary condition at the surface because

$$(K_e\theta)_{z=0} = \left(k\frac{\partial \theta}{\partial z}\right)_{z=0} \tag{6}$$

The other boundary conditions are

$$\theta = 0 \quad \text{at} \quad z = \infty \tag{7}$$

$$\theta = 0 \quad \text{at} \quad x = \pm \infty \tag{8}$$

$$\theta = 0 \quad \text{at} \quad y = \pm \infty \tag{9}$$

Note that x = 0, y = 0 is the center of the repository plane.

Solution of Equation

Equation 5 is solved by the method of Green's functions for an instantaneous heat source (Ref. 3), later generalized for a continuous heat source. For a unit instantaneous heat source of 1 joule, the solution to Equation 5 in terms of Green's functions G_x, G_y, and G_z for the given boundary conditions can be written:

$$\theta_f = G_x\, G_y\, G_z \tag{10}$$

The Green's functions are expressed

$$G_x = \frac{1}{2L}\left\{\text{erf}\left[\frac{(\frac{L}{2} + x)}{\sqrt{4kt}}\right] + \text{erf}\left[\frac{(\frac{L}{2} - x)}{\sqrt{4kt}}\right]\right\} \tag{11}$$

$$G_y = \frac{1}{2b}\left\{\operatorname{erf}\left[\frac{\left(\frac{W}{2}+y\right)}{\sqrt{4kt}}\right] + \operatorname{erf}\left[\frac{\left(\frac{W}{2}-y\right)}{\sqrt{4kt}}\right]\right\} \tag{12}$$

$$G_z = \frac{1}{2\sqrt{\pi kt}}\left(e^{-(z-z')^2/4kt} + e^{-(z+z')^2/4kt}\right)$$

$$- h\, e^{\{k\ t\ h^2+h(z+z')\}}\ \operatorname{erfc}\left\{\frac{z+z'}{2\sqrt{kt}} + h\sqrt{kt}\right\} \tag{13}$$

(Ref. 3, p. 358)

where $h = \frac{K_e}{k}$.

The temperature for a continuous source can be generalized with the convolution integral

$$\theta = \int_0^t \theta_1(\tau)\, H(t-\tau)\, d\tau \tag{14}$$

where $H(t-\tau)$ = heat generation rate of the repository at time = $(t-\tau)$.

Equation 14 is solved by numerical integration using Simpson's rule quadrature, and with a change in the independent variable $t = p^2$ to eliminate the singularity in G_z at t=0. The heat rate H(t) is expressed as a tabular function with linear interpolation. A simple BASIC Language computer program to calculate temperature is given in Appendix A.

Discussion

The choice of the z-direction Green's function was dictated by the boundary condition at the earth's surface with heat transfer to the atmosphere. Calculations of repository temperature using typical values of coefficients

for HLW repositories and atmospheric heat transfer quickly demonstrated that the z-direction Green's function degenerated to an asymptotic form:

$$G_z = \frac{1}{2\sqrt{\pi kt}} \{e^{-(z-z')^2/4kt} - e^{-(z+z')^2/4kt}\} \tag{15}$$

This form of Green's function does not contain the coefficient h at all, and is in fact the Green's function for the boundary condition:

$$\theta = 0 \quad \text{at} \quad z = 0 \, . \tag{16}$$

Therefore, heat transfer at the atmospheric boundary must be very efficient compared to the conduction of heat through the ground for typical HLW repository conditions.

This conclusion is not very surprising if one considers what the temperature of a repository with the same thermal loading per square meter of surface area would be in air rather than rock. At steady state, the heat emanating from the waste would balance the heat flux to the atmosphere:

$$K_e \theta = H$$

or

$$\theta = H/K_e \tag{17}$$

If the initial heat loading of the repository were 4.41×10^8 j/(m^2-yr) and the estimated K_e were 2.87×10^8 j/(m^2-yr-°C), then

$$\theta < 1.54°C \, .$$

The fact that the waste decays with time and that it is buried deep underground would therefore indicate that the temperature elevation at the surface of the earth would be very small, and for all intents and purposes, the boundary condition, Equation 16 can be used.

The computer program therefore employs the z-direction Green's function given in Equation 15.

The usefulness of the model will be demonstrated by using it to explore the sensitivity of temperature to various modeling assumptions.

Effects of Model Dimensionality on Maximum Repository Temperature

The sensitivity of temperature at the repository plane to the choice of a 1-, 2-, or 3-dimensional model can be illustrated. For the present example, the repository has the characteristics, presented in Table 1, which are typical of a basalt repository for spent fuel, taken from Ref. 4.

Table 1 - Parameters for HLW repository example

Repository dimensions:
length = 1600 m
width = 1200 m

Depth of repository = 1200 m

Heat capacity of rock = 2.77×10^6 j/(m^3-°C)

Conduction coefficient of rock = 7.25×10^7 j/(m-yr-°C)

Heat load per square meter of repository:
initial heat load = 4.41×10^8 j/(m^2-yr)

Time (year)	Relative heat load
0	1
5	0.826
10	0.706
15	0.639
20	0.588
30	0.497
40	0.424
50	0.384
70	0.281
100	0.214
190	0.135
290	0.105
390	0.088
490	0.0773
990	0.0451
1,990	0.0236
5,990	0.0129
9,990	0.011
50,000	0.00477
100,000	0.00215

Figure 2 shows the maximum temperature at the center of the repository, $x = 0$, $y = 0$, $z = z'$ as a function of time. Also plotted in Figure 2 are the temperatures for a 2-dimensional (x-z) model of a repository which is infinitely long in the y direction, and a 1-dimensional (z) model which is infinite in both the x and y directions. All three models have the same heat generation rate per unit surface area, and predict a maximum repository temperature of about 63°C at t = 60 years. The maximum repository temperature in fact is nearly the same for all the models until about t = 1,000 years, at which time the modeled temperatures diverge. The 1- and 2-dimensional models predict higher repository temperatures because the heat transfer in the missing dimensions is neglected.

An analytical expression for maximum repository temperature was developed in Ref. 1.

$$\theta_{max} = \frac{0.54104\ H_o}{\rho C_p \sqrt{k\sigma\lambda}} \quad \text{at} \quad t = 0.854/\lambda \qquad (18)$$

where λ is the presumed exponential decay rate of the radioactive waste. The waste does not decay as a whole exponentially, however, because it is a complicated mixture of many radionuclides. Since most of the heat for short times (<100 years) comes for Sr-90 and Cs-137, which have half-lives of about 30 years, an approximation of λ can be made:

$$\lambda = \frac{\ln 2}{30\ \text{years}} = 0.0231/\text{year}$$

For $H_o = 4.41 \times 10^8$ joules/m^2-year therefore,

$$\theta_{max} = 62.5°C \quad \text{at} \quad t = 37\ \text{years}.$$

The maximum temperature is close to that calculated for the time-dependent model, although the time that the peak is reached is somewhat shorter than for the time-dependent model.

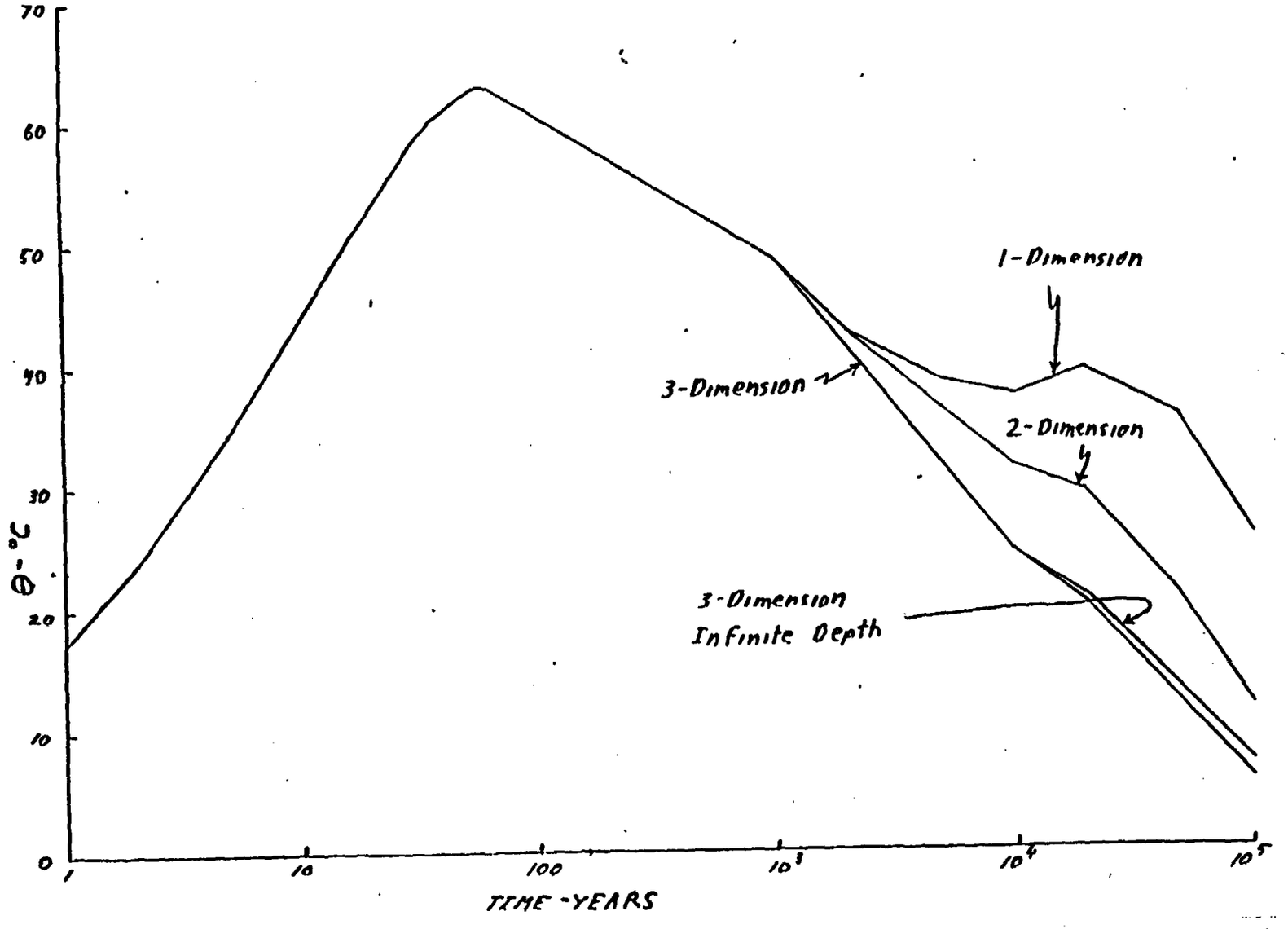

FIGURE 2 - MAXIMUM TEMPERATURE IN CENTER OF REPOSITORY

Effect of the Boundary at Earth's Surface on Repository Temperature

The effect of a constant temperature boundary, $\theta = 0$ at $z = 0$ is demonstrated in Figure 2. The temperature in the center of the repository, $x = 0$, $y = 0$, and $z = z'$ calculated with the boundary condition $\theta = 0$ at $z = 0$, $z' = 1200$ m is compared to the same case, but for $\theta = 0$ at $z = 0$ for $z' = 10^5$ m (essentially, $z' = \infty$). Only a very slight difference between the two cases is evident, and only for long times, greater than about 10,000 years.

Effects of Model Dimensionality and Boundary Conditions on the 10°C Isotherm

The position of the maximum 10°C isotherm surrounding the respository will be more greatly affected by the model dimensionality and boundary conditions than would the maximum repository temperature. Figure 3 illustrates the approximate extent of the 10°C isotherms at $t = 10{,}000$ years for some of the cases treated in the previous section.

The bold line represents the 10°C isotherm calculated with the 3-dimensional model with correct surface boundary condition for repository temperature along the plane $y = 0$ at $t = 10{,}000$ years. The thin solid line is for the same case, but for a two-dimensional approximation to the repository (i.e., an infinite strip source in the y direction). The 10°C isotherm extends considerably farther in this case, because heat cannot escape in the y direction.

The dotted line illustrates the 10°C isotherm for a repository in an infinite vertical medium, without the influence of the boundary condition $\theta = 0$ at $z = 0$. Only a relatively small error would be made by neglecting the surface boundary condition for the 10°C isotherm, although there would be progressively greater effects on lower temperatures for long times.

Conclusions

A 3-dimensional analytical model for heat transfer in a HLW repository in a uniform medium has been developed. The model is useful for investigating the importance of certain assumptions used in other numerical and analytical

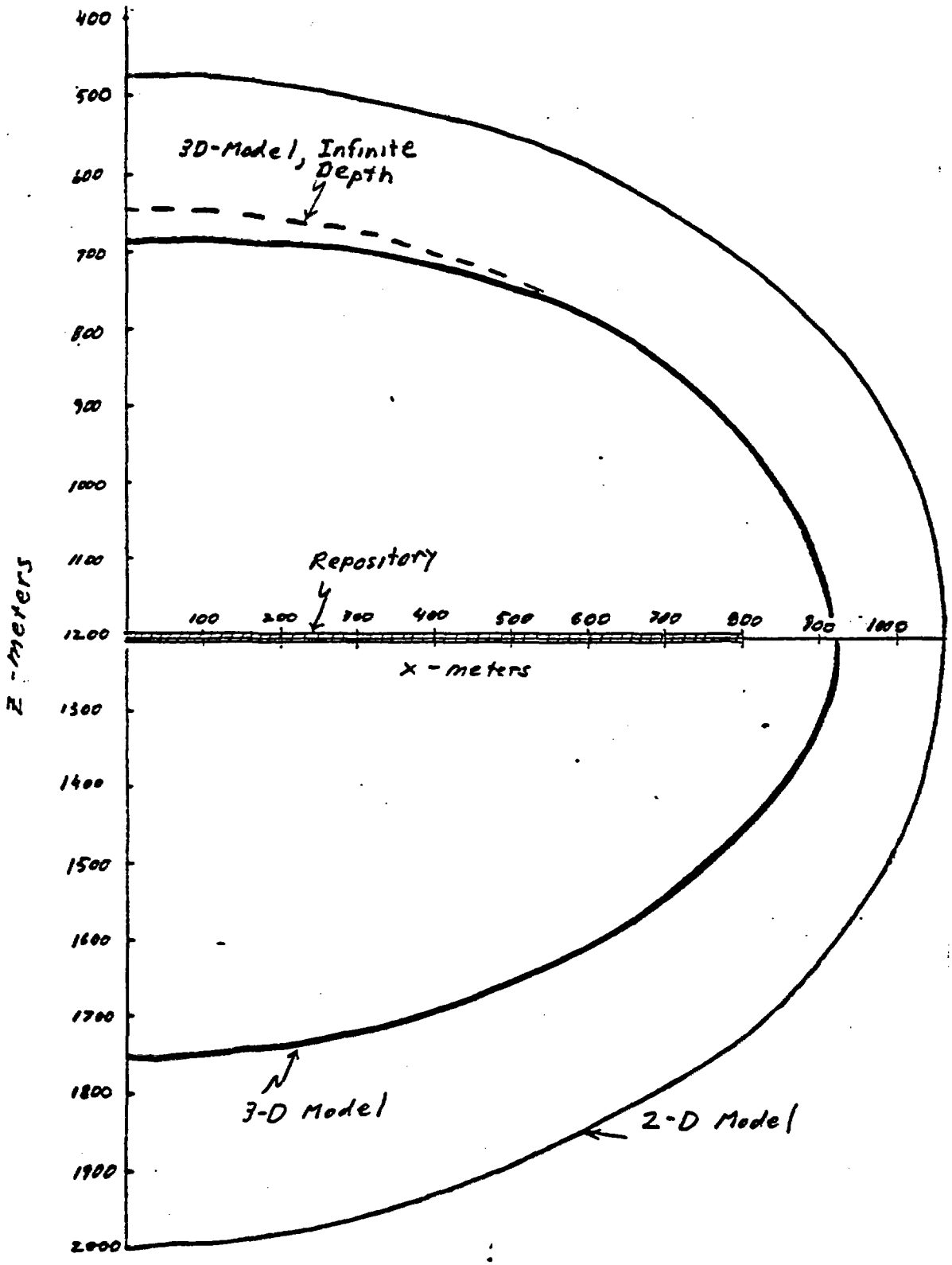

FIGURE 3 - POSITION OF 10 DEGREE C ISOTHERM AT 1000 YEARS

models. The model takes advantage of a previously determined conclusion that in many repository situations, heat transfer by conduction through rock would be much larger than heat transfer caused by flowing groundwater.

Several conclusions can be drawn as a result of exercises performed with the model using parameters and coefficients typical of the Basalt Waste Isolation Project (BWIP):

1. The temperature close to the center of the repository is very insensitive to the choice of model dimensionality (i.e., 1, 2, or 3 dimensions) or boundary conditions (i.e., surface of earth), except at very long times, greater than about 1,000 years. The temperature maximum near the center of the repository would occur in less than 100 years for a 10-year-old spent fuel heat source.

2. Although maximum temperatures close to the repository can be estimated by considering short-lived isotopes, temperatures for long times and far from the source must include the long-lived components of the heat source.

3. The temperature maximum very close to the repository can be closely predicted by considering only short-lived isotopes such as Sr-90 and Cs-137, using a 1-dimensional analytical model of the repository in an infinite medium. This conclusion is important because such a model assumption was made in Ref. 1 to predict the relative importance of conductive to convective heat transfer in a HLW repository, which led to the justification for ignoring convective heat transfer.

4. Heat transfer at the surface of the earth is very efficient compared to conduction through the earth. This observation leads to the conclusion that the boundary condition at the surface of the earth can be T = constant instead of a boundary condition including heat transfer to the atmosphere.

5. The maximum penetration of isotherms into the rock will be overestimated if a 2-dimensional model is used instead of a 3-dimensional model. This error is on the order of 100-200 meters for the maximum 10°C isotherm penetration in the sample investigated, and would be larger for lower temperature isotherms at long times.

The model is useful and efficient, although it is limited to simple geometries and uniform thermal conductivity and heat capacity. It allows investigation of heat transfer with very little computation even for very long times, whereas a numerical model would require large computational resources and long run times. The model may be useful for defining the shape of isotherms for the disturbed-zone concept, or may be used to generate temperatures for further analyses of phenomena near the repository. Since the model ignores heat transfer by convection, the validity of this assumption for each case should be checked using the guidance of Ref. 1.

References

1. R. Codell, Memorandum and attachment for M. R. Knapp, "Convective Heat Transfer in HLW Repository - Disturbed Zone Task," February 8, 1984, Geotechnical Branch, Division of Waste Management, USNRC, Washington, DC 20555.

2. D. K. Brady, W. L. Graves and J. C. Geyer, "Surface Heat Exchange at Power Plant Cooling Lakes," Report No. 5, Edison Electric Institute, EEI publication 69-401, New York, NY, 1969.

3. H. S. Carslaw and J. C. Jaeger, Conduction of Heat In Solids, Oxford University Press, London, 1959.

4. M. Gordon and M. Weber, "Non-Isothermal Flow Modeling of the Hanford Site," March 1983 Internal Division of Waste Management report, USNRC, Washington, DC 20555.

Appendix - Program HLWTEMP

The BASIC language computer program described in the text is listed in Figure A2. It is set up to run on the NRC MV-8000, taking advantage of the BAS compiler for speed.

The HLWTEMP program calculates temperature in a 1-, 2-, or 3-dimensional semi-infinite medium, caused by heat generation from a rectangular thin plate source of length L, width W, and depth z' below the earth's surface. Boundary conditions are $\theta = 0$ at $z = 0$, $\theta = 0$ at $x = \pm \infty$, $\theta = 0$ at $y = \pm \infty$, $\theta = 0$ at $z = \infty$, where θ is the temperature above ambient rock temperature. Heat load per unit area of the plate is defined as a function of time by linear interpolation from a table. Heat capacity and thermal conductivity of the rock must be constants.

Temperature θ is calculated and displayed on a rectangular grid defined by the user, in the x-z plane, along a constant y value.

Running Program HLWTEMP

Program HLWTEMP is interactive and prompts the user for the necessary information. The heat load time-dependency is specified by the DATA statements in the program for 10-year old spent fuel, although the initial heat load per square meter is input to the program when run. A different time-dependency can be specified by changing the relative power vs. time table in the DATA statements on lines 400 to 460 and recompiling the program. Up to 30 table values can be specified. The integration interval is presently set to 50 steps/temperature calculation in line 660. This value can be increased for a more complicated heat table at the expense of run time.

Program output is set up for a 132-column printer (e.g., DECWRITER), and is limited to 11 columns of x values. For an 80-column printer, the output should be limited to 7 columns of x values by changing the following statements:

1. line 770, eliminate PS(8) through PS(11)
2. line 1170, eliminate PS(8) through PS(11)

Use of the program is illustrated by the example presented below:

Example - Basalt repository

Calculate the temperature along the plane y = 0 at t = 1,000 years for the repository having the characteristics given in Table 1. Print the results on a grid which is 100 m between points in both the x and z directions, for x = 0 (centerline) to x = 1000 m and z = 700 m to 1800 m. The results of the run are shown in Figure A1. Note that the program terminates for a negative input of time.

Access to the MV8000 directory containing the BASIC and compiled versions of the program can be obtained from Richard Codell.

```
 X HLWTEMP

 REPOSITORY HEAT TRANSFER MODEL USING
 GREEN'S FUNCTION SOLUTION TO HEAT TRANSFER FROM RECTANGULAR PLATE
 R CODELL US NUCLEAR REGULATORY COMMISSION, WASH DC 20555
ENTER 3(XYZ),2(XZ), OR 1(Z) DIMENSIONS
? 3
ENTER K, JOULES/M/YR/DEG C
? 7.25E7
ENTER HEAT CAPACITY OF ROCK,JOULES/CU M/DEG C
? 2.77E6
ENTER INITIAL HEAT LOAD, JOULES/SQ M/YR
? 4.41E8
INPUT LENGTH(X),WIDTH(Y),DEPTH(Z) OF REPOSITORY
? 1600,1200,1200
INPUT X0 AND DX, METERS AND NO OF X PRINTS
? 0,100,11
ENTER Z0,DZ, METERS AND NO OF Z PRINTS
? 700,100,12
INPUT Y METERS
? 0
ENTER TIME,YRS
? 1000
```

	X-METERS									
	0	100	200	300	400	500	600	700	800	900	1000
Z-METERS											
700	1.62	1.62	1.62	1.61	1.57	1.49	1.34	1.10	.81	.52	.29
800	4.47	4.47	4.46	4.42	4.33	4.12	3.70	3.05	2.23	1.42	.76
900	10.36	10.35	10.34	10.27	10.07	9.60	8.66	7.14	5.18	3.22	1.70
1000	20.37	20.36	20.33	20.22	19.88	19.03	17.28	14.26	10.19	6.11	3.10
1100	34.17	34.16	34.11	33.95	33.47	32.26	29.61	24.66	17.09	9.51	4.56
1200	48.85	48.84	48.79	48.61	48.07	46.69	43.62	37.51	24.43	11.34	5.23

FIGURE A1 - OUTPUT OF HLWTEMP PROGRAM FOR EXAMPLE

1300	34.17	34.16	34.11	33.95	33.47	32.26	29.61	24.66	17.09	9.51	4.56
1400	20.37	20.36	20.33	20.22	19.88	19.03	17.28	14.26	10.19	6.11	3.10
1500	10.36	10.35	10.34	10.27	10.07	9.60	8.66	7.14	5.18	3.22	1.70
1600	4.47	4.47	4.46	4.42	4.33	4.12	3.70	3.05	2.23	1.42	.76
1700	1.62	1.62	1.62	1.61	1.57	1.49	1.34	1.10	.81	.52	.29
1800	.50	.50	.49	.49	.48	.45	.41	.34	.25	.16	.09

```
ENTER TIME,YRS
? -1

STOP
```

```
00100 REM GREEN'S FUNCTION SOLUTION FOR HEAT TRANSFER FROM A
00110 REM RECTANGULAR THIN PLATE IN A SEMIINFINITE UNIFORM MEDIUM.
00120 REM PLATE IS PARALLEL TO EARTH'S SURFACE AND A DEPTH Z1 METERS.
00130 REM LENGTH(X DIRECTION) IS L5 METERS, WIDTH(Y DIRECTION) IS
00140 REM W5 METERS.
00150 REM.INITIAL HEAT LOAD IS H0 JOULES/SQ METER/YEAR.
00160 REM TIME DEPENDENCE OF HEAT IS SPECIFIED BY TH AND H TABLE
00170 REM IN DATA STATEMENTS BELOW. LINEAR INTERPOLATION
00180 REM BETWEEN TABLE POINTS IS USED.
00190 REM HEAT CAPACITY CR IS SPECIFIED IN JOULES/CU METER/DEG C.
00200 REM THERMAL CONDUCTIVITY K IS SPECIFIED IN JOULES/METER/DEG C/YR.
00210 REM NOTE: PROGRAM IS SET UP FOR 132 COL PRINTER.
00220 REM FOR 80 COLUMN PRINTER YOU SHOULD CHANGE PRINT USING STATEMENTS.
00230 REM PROGRAM SHOULD BE SAVED AND COMPILED WITH THE BAS COMPILER
00240 REM BEFORE USING SINCE IT WOULD BE TOO SLOW OTHERWISE.
00250 PRINT
00260 PRINT " REPOSITORY HEAT TRANSFER MODEL USING"
00270 PRINT " GREEN'S FUNCTION SOLUTION TO HEAT TRANSFER FROM RECTANGULAR P
LATE"
00280 PRINT " R CODELL US NUCLEAR REGULATORY COMMISSION, WASH DC 20555"
00290 PRINT "ENTER 3(XYZ),2(XZ), OR 1(Z) DIMENSIONS"
00300 INPUT D123
00310 MARGIN 132
00320 DIM H(30),TH(30),PS(12)
00330 LET N7=11
00340 READ N
00350 FOR I=1 TO N
00360   READ TH(I),H(I)
00370 NEXT I
00380 REM TH(I) IS TIME, H(I) IS CORRESPONDING RELATIVE HEAT LOAD
00390 REM H AT TH=0 SHOULD ALWAYS BE 1
00400 DATA 20
00410 REM TABLE FOR 10 YEAR OLD SPENT FUEL RELATIVE HEAT
00420 DATA 0,1,5,.826,10,.706,15,.639,20,.588,30,.497
00430 DATA 40,.424,50,.384,70,.281,100,.214,190,.133
00440 DATA 290,.105,390,.088,490,.0773,990,.0451
00450 DATA 1990,.0236,5990,.0129,9990,.011
00460 DATA 50000,.00477,100000,.00215
00470 PRINT "ENTER K, JOULES/M/YR/DEG C"
00480 INPUT KM
00490 PRINT "ENTER HEAT CAPACITY OF ROCK,JOULES/CU M/DEG C"
00500 INPUT RC
00510 PRINT "ENTER INITIAL HEAT LOAD, JOULES/SQ M/YR"
00520 INPUT H0
00530 PRINT "INPUT LENGTH(X),WIDTH(Y),DEPTH(Z) OF REPOSITORY"
00540 INPUT L5,W5,Z1
00550 PRINT "INPUT X0 AND DX, METERS AND NO OF X PRINTS"
00560 INPUT X0,DXP,NPX
00570 PRINT "ENTER Z0,DZ, METERS AND NO OF Z PRINTS"
00580 INPUT Z0,DZP,NPZ
00590 PRINT "INPUT Y METERS"
00600 INPUT Y
00610 LET C7=H0/RC
00620 LET C8=1/SQR(3.14159*KM/RC)
00630 LET K3=KM/RC
```

FIGURE A2 - HLWTEMP PROGRAM LISTING

```
00640 REM NT IS NO OF INTEGRATION STEPS  TYP 50
00650 REM - MAY INCREASE FOR COMPLICATED HEAT TABLE
00660 LET NT=50
00670 PRINT "ENTER TIME,YRS"
00680 INPUT T1
00690 REM - TERMINATE ON NEGATIVE TIME INPUT
00700 IF T1<0 THEN STOP
00710 FOR IX=1 TO 12
00720   LET PS(IX)=(IX-1)*DXP+X0
00730 NEXT IX
00740 PRINT
00750 PRINT "                                        X-METERS"
00760 REM SETUP FOR 132 COLUMN PRINTER. FOR 80 COL ELIMINATE PS(8) ON
00770 PRINT USING 00840:PS(1),PS(2),PS(3),PS(4),PS(5),PS(6),PS(7),PS(8),PS(
9),PS(10),PS(11)
00780 FOR IX=1 TO 12
00790   LET PS(IX)=0
00800 NEXT IX
00810 PRINT
00820 PRINT "Z-METERS"
00830 FOR IZ=1 TO NPZ
00840   IMAGE :           #####     #####     #####     #####     #####
#####    #####     #####     #####     #####     #####     #####
00850   LET Z=(IZ-1)*DZP+Z0
00860   FOR IX=1 TO NPX
00870     LET X=(IX-1)*DXP+X0
00880     LET SK=SQR(4*K3)
00890     LET R1=(.5*L5+X)/SK
00900     LET R2=(.5*L5-X)/SK
00910     LET R3=(.5*W5+Y)/SK
00920     LET R4=(.5*W5-Y)/SK
00930     LET C1=(Z-Z1)^2/(4*K3)
00940     LET C2=(Z1+Z)^2/(4*K3)
00950     LET C5=(Z+Z1)/(2*SQR(K3))
00960     LET P=0
00970     REM TRANSFORM INDEPENDENT VARIABLE
00980     LET S3=SQR(T1)
00990     LET DT=S3/NT
01000     LET D5=DT/2
01010     LET D6=DT/6
01020     LET T=0
01030     LET F=0
01040     REM BEGIN SIMPSON'S RULE
01050     FOR I=1 TO NT
01060       LET F1=F
01070       LET T=T+D5
01080       GOSUB 01270
01090       LET F2=F
01100       LET T=T+D5
01110       GOSUB 01270
01120       LET P=P+(F1+4*F2+F)*D6
01130     NEXT I
01140     LET PS(IX)=P
01150   NEXT IX
01160   REM NOTE: SETUP FOR DECWRITER 132 COL   FOR 80 COL, ELIMINATE PS(8)
 ON
```

```
01170   PRINT USING 01180:Z,PS(1),PS(2),PS(3),PS(4),PS(5),PS(6),PS(7),PS(8)
,PS(9),PS(10),PS(11)
01180   IMAGE :#####      ##.##      ##.##      ##.##      ##.##      ##.##
##.##      ##.##      ##.##      ##.##      ##.##      ##.##      ##.##
01190   PRINT
01200   PRINT
01210   PRINT
01220   PRINT
01230   PRINT
01240 NEXT IZ
01250 GOTO 00670
01260 REM BEGIN LINEAR INTERPOLATION OF HEAT TABLE
01270 LET T2=T1-T*T
01280 FOR J=1 TO N-1
01290   IF TH(J+1)>T2 THEN GOTO 01330
01300 NEXT J
01310 IF T2<=0 THEN LET J=1
01320 IF T2<0 THEN LET T2=0
01330 LET H1=H(J)+(T2-TH(J))/(TH(J+1)-TH(J))*(H(J+1)-H(J))
01340 REM CALCULATE GREEN'S FUNCTIONS
01350 LET T6=T*T
01360 LET A1=C1/T6
01370 LET G1=0
01380 IF A1<85 THEN LET G1=EXP(-A1)
01390 LET A2=C2/T6
01400 LET G2=0
01410 IF A2<85 THEN LET G2=EXP(-A2)
01420 LET A=R1/T
01430 GOSUB 01660
01440 LET E1=S
01450 LET A=R2/T
01460 GOSUB 01660
01470 LET E2=S
01480 LET A=R3/T
01490 GOSUB 01660
01500 LET E3=S
01510 LET A=R4/T
01520 GOSUB 01660
01530 IF D123=3 THEN GOTO 01620
01540 IF D123=2 THEN GOTO 01590
01550 REM GX*GY FOR 1-D
01560 LET GXY=1
01570 GOTO 01640
01580 REM GX*GY FOR 2-D
01590 LET GXY=.5*(E1+E2)
01600 GOTO 01640
01610 REM GX*GY FOR 3-D
01620 LET GXY=.25*(E1+E2)*(E3+S)
01630 REM KERNAL OF INTEGRAL
01640 LET F=H1*C7*C8*(G1-G2)*GXY
01650 RETURN
01660 REM ERROR FUNCTION
01670 LET K8=ABS(A)
01680 LET K9=1/(1+.47047*K8)
01690 LET S=.348024*K9-9.58798E-02*K9*K9+.747856*K9^3
```

```
01700 LET K9=0
01710 IF K9>7 THEN GOTO 01730
01720 LET K9=EXP(-K8*K8)
01730 LET S=1-S*K9
01740 IF A>0 THEN RETURN
01750 LET S=-S
01760 RETURN
01770 END
```